HHS Public Access

Author manuscript

Nat Cell Biol. Author manuscript; available in PMC 2015 November 01.

Published in final edited form as:

Nat Cell Biol. 2015 May ; 17(5): 665–677. doi:10.1038/ncb3158.

The ITIM-containing receptor LAIR1 is essential for acute myeloid leukemia development

Xunlei Kang[1], **Zhigang Lu**[1], **Changhao Cui**[1], **Mi Deng**[1], **Yuqi Fan**[1], **Baijun Dong**[3], **Xin Han**[4], **Fuchun Xie**[5], **Jeffrey W. Tyner**[6], **John E. Coligan**[7], **Robert H. Collins**[2], **Xiangshu Xiao**[5], **M. James You**[3,8], and **Cheng Cheng Zhang**[1,9]

[1]Departments of Physiology and Developmental Biology, University of Texas Southwestern Medical Center, Dallas, Texas 75390

[2]Internal Medicine, University of Texas Southwestern Medical Center, Dallas, Texas 75390

[3]Department of Hematopathology, University of Texas MD Anderson Cancer Center, Houston, TX 77030-4009

[4]Department of Laboratory Medicine, Division of Pathology and Laboratory Medicine, University of Texas MD Anderson Cancer Center, Houston, TX 77030-4009

[5]Department of Physiology and Pharmacology, Oregon Health and Science University Knight Cancer Institute, Portland, OR 97239

[6]Cell and Developmental Biology, Oregon Health and Science University Knight Cancer Institute, Portland, OR 97239

[7]Receptor Cell Biology Section, National Institute of Allergy and Infectious Diseases, NIH, Rockville, MD 20852

[8]The University of Texas Graduate School of Biomedical Sciences at Houston, Houston, TX 77030

Summary

Conventional strategies are not particularly successful in treatment of leukemia, and identification of signaling pathways crucial to the activity of leukemia stem cells will provide targets for the development of new therapies. Here we report that certain receptors containing the immunoreceptor tyrosine-based inhibition motif (ITIM) are crucial for the development of acute myeloid leukemia (AML). Inhibition of expression of the ITIM-containing receptor LAIR1 does

[9]Correspondence should be addressed to: Cheng Cheng Zhang, Telephone (214) 645-6320, Fax (214) 648-1960, Alec.Zhang@UTSouthwestern.edu.

Contributions: X.K. performed most of the experiments, analysed data and contributed to writing the paper; Z.L. performed the TCGA and clustering analyses; C.C. performed the CAMK experiments; M.D. performed the LILRB knockdown experiments. Y.F., F.X., and X.X. performed the CREB inhibitor experiments and provided advice; B.D., X.H., R.H.C., and M.J.Y. collected the primary AML samples and provided advice; J.W.T. helped experiments using leukemia cell lines and contributed to paper writing; J.E.C. provided LAIR1 deficient mice and contributed to paper writing; C.C.Z. conceived, coordinated and supervised the project, designed experiments, analysed data and wrote the paper.

Competing financial interests: The authors declare no competing financial interests.

not affect normal hematopoiesis but abolishes leukemia development. LAIR1 induces activation of SHP-1, which acts as a phosphatase-independent signaling adaptor to recruit CAMK1 for activation of downstream CREB in AML cells. The LAIR1/SHP-1/CAMK1/CREB pathway sustains the survival and self-renewal of AML stem cells. Intervention in the signaling initiated by ITIM-containing receptors such as LAIR1 may result in successful treatment of AML.

Introduction

Leukemias are malignant blood diseases characterized by uncontrolled overproduction of hematopoietic progenitors or terminally differentiated leukocytes. Acute myeloid leukemia (AML) is the most common adult acute leukemia. Acute lymphoblastic leukemia (ALL) is the most common malignancy in children and is also diagnosed in adults. Current chemotherapies are not particularly successful in treating AML and some ALL. For example, despite continuous treatment, the majority of the AML patients relapse within 5 years [1]. It has been suggested that leukemia stem cells, a small population of stem-like cancer cells that have the capacity for indefinite self-renewal [2, 3], are responsible for initiation and relapse. To effectively inhibit the activity of leukemia stem cells and treat acute leukemia, new molecular targets and therapeutic approaches need to be identified.

It is hypothesized that leukemia stem cells reside in a bone marrow microenvironment or niche and play an important role in regulation of initiation, differentiation, migration, and chemoresistance of leukemia [4-6]. In addition, systematic inflammatory and oxidative factors are critical extrinsic factors for leukemia development [7]. Specific surface receptors on leukemia cells presumably interact with the extrinsic environment and regulate the fates of leukemia cells through unique signaling pathways. These include tyrosine kinase receptors [8], cytokine receptors [9], chemokine receptors [10], adhesion molecules and integrins (such as CD44, CD49d, integrin beta 3, CD47, CD96, CD33) [11-16], Notch [17], Wnt receptors [18, 19], Smoothened [20], receptors for TGF-beta family [21], and other surface molecules. Some of these receptors mediate signaling that differs in leukemia cells from that in normal hematopoietic cells, which should enable the development of novel anti-leukemia strategies [4, 16, 22-24].

In our attempt to identify stem cell and leukemia related surface receptors, we isolated human leukocyte immunoglobulin (Ig)-like receptor B2 (LILRB2) and mouse paired Ig-like receptor (PirB) as receptors for angiopoietin-like proteins (Angptls) [25]. These receptors contain immunoreceptor tyrosine-based inhibitory motifs (ITIM) in their intracellular domains and are classified as inhibitory receptors because ITIM motifs can recruit phosphatases like SHP-1, SHP-2, and SHIP to negatively regulate cell activation [26-28]. We showed that PirB is expressed on AML cells and required for AML development in mouse leukemia models [25]. Nevertheless, it is unknown whether ITIM-receptors have direct effects on leukemia cells.

Here we demonstrated that some ITIM-receptors are expressed on leukemia cells and directly support leukemia development. We further discovered a signaling pathway initiated from the LAIR1, a representative ITIM-receptor. This identified ITIM-receptor signaling pathway may represent an ideal target for AML treatment. Our demonstration that some

ITIM-receptors are not “inhibitory” but supportive of leukemia development will alter the current understanding of the mechanisms of cancer pathogenesis, cell signaling, and therapeutic approaches.

Results

The expression of some ITIM-receptors inversely correlates with AML development

To identify potential surface receptor genes that support leukemia development, we performed an *in silico* analysis of the relationship between gene expression and the overall survival of AML patients. To our surprise, while the expression of 2 out of 58 ITIM-receptors positively correlated with the overall survival of acute myeloid leukemia (AML) patients, 20 of these receptors had negative correlation between expression and survival (Supplementary Fig. 1a, Supplementary Table 1). To determine the functions of these ITIM-receptors, we inhibited expression of these receptors individually in human leukemia cell lines using lentivirus-encoded small hairpin RNAs (shRNAs) and found that cell growth was blocked when expression of certain receptors was silenced (Fig. 1A, Supplementary Fig. 1b). These results suggest that some ITIM-receptors directly support human leukemia cell growth.

LAIR1 is essential for the growth of human acute leukemia cells

Based on the shRNA knockdown screening, we selected LAIR1 as a representative ITIM-receptor that does not affect normal hematopoiesis [29] but is essential for leukemia development (Fig. 1A, Supplementary Fig. 4) for further mechanistic study. LAIR1 is a type I transmembrane glycoprotein containing one extracellular Ig-like domain that binds collagens or surfactant protein D [30] and two intracellular ITIMs that recruit SHP-1 and SHP-2. LAIR1 is known to be expressed on various lineages of hematopoietic cells and hematopoietic progenitor $CD34^+$ cells [31]. Our study suggests that collagens, but not the surfactant protein D, are major ligands for LAIR1 in the hematopoietic system (Supplementary Fig. 1e-g). Crosslinking of LAIR1 via antibodies delivers an inhibitory signal to some immune cells *in vitro* [29, 31, 32]; however, as *lair1*-null mice have no overt defects in hematopoiesis, the biological function of LAIR1 *in vivo* remains unresolved [29]. Flow cytometry analysis indicated that LAIR1 is highly expressed on a number of human acute leukemia cell lines, including MV4-11 (AML), THP-1 (AML), U937 (AML), 697 (B-ALL), Kasumi2 (B-ALL), and RCH-ACV (B-ALL), but not on K562 (Fig. 1B).

To study the potential function of LAIR1 in human leukemia, we silenced the expression of *lair1* by introducing lentivirus-encoded shRNAs into human leukemia lines. All three shRNAs tested efficiently decreased total and surface expression of LAIR1 (Fig. 1C-D) and essentially blocked the *in vitro* growth of each of those leukemia lines that express surface LAIR1 (Fig. 1E, I and J, Supplementary Fig. 2a). By contrast, knockdown of *lair1* did not influence growth of K562 cells (Supplementary Fig. 2b). We further validated shRNA-226 as a *lair1* specific shRNA (Fig. 1F-G) and used it in subsequent experiments.

To determine the underlying mechanism by which LAIR1 supports leukemia cell growth, we found that LAIR1 knockdown did not alter the cell cycle status but dramatically increased apoptosis of leukemia cells (Fig. 1H, Supplementary Fig. 2c).

Next we tested whether inhibition of *lair1* expression alters *in vivo* engraftment of MV4-11 and 697 leukemia cells in transplanted NOD/SCID-IL2RG (NSG) mice. Transplantation with cells deficient in *lair1* diminished leukemia development (Fig. 2A-E and Supplementary Figs. 2 d-e and 3). Very few GFP^+ cells, which mark the lentivirus-infected human cells, were observed in mice transplanted with cells that expressed the shRNA targeting *lair1* compared to controls. Critically, the observed GFP^+ cells in the groups transplanted with cells treated with shRNA targeting *lair1* did express surface LAIR1 (Fig. 2A-B), suggesting that cells in which the shRNA was lost but GFP retained might have been selected. A further sorting of different cell populations followed by real-time PCR indicates that GFP^+ $LAIR1^{high}$ cells in the LAIR1 shRNA 226 knockdown samples isolated from the transplanted NSG mice contain much less LAIR1 shRNA than the original GFP^+ $LAIR1^{low}$ counterparts before transplantation (Supplementary Fig. 2d). Therefore LAIR1-expressing leukemia cells successfully engrafted mice; but if there was no surface expression of LAIR1, the cells failed to engraft. Similar results were obtained in B-ALL 697 cells (Fig. 2C-D). The effects of *lair1* silencing on the *in vitro* growth and *in vivo* development of leukemia cells are summarized in Fig. 1K. These results clearly indicate that LAIR1 is essential for growth of these human AML and ALL leukemia cell lines.

LAIR1 supports mouse AML development during serial transplantation

To gain a deeper understanding of the mechanism by which LAIR1 supports AML development, we analyzed AML development in *lair1*-null mice [29]. These mice have normal hematopoiesis and normal $Lin^-Sca\text{-}1^+Kit^+$ percentages in the BM [29]. There was no difference in repopulation or homing between *lair1*-null and WT HSCs (Supplementary Fig. 4a-e).

We used several retrovirus transplantation models including MLL-AF9 (AML) [25, 33, 34], AML1-ETO9a (AML) [35], and N-Myc (B-ALL) [36] to study the role of LAIR1 in leukemia development. Whereas there was no significant difference in AML development upon primary transplantation of 100,000 infected WT and *lair1*-null cells (Supplementary Fig. 4a-b), the mice transplanted with MSCV-MLL-AF9-IRES-YFP transduced *lair1*-null cells developed AML much more slowly than controls in secondary transplantation (Fig. 3A-E). The gradual decrease of YFP^+ *lair1*-null cells in most mice and the occasional spontaneous increase in numbers of YFP^+ cells in a few mice (Fig. 3C) suggests that the *lair1*-null AML cells indeed successfully engrafted into these recipient mice upon transplantation. We performed this experiment independently seven times by using different and pooled bone marrow (BM) samples (Supplementary Fig. 5c-d), and all experiments gave similar results.

Consistent with data from the MLL-AF9 model, the deficiency of *lair1* in the AML1-ETO9a AML model [35] and in the N-Myc B-ALL model [36] also largely eliminated the disease during secondary transplantation (Fig. 3F-G, Supplementary Fig. 5e-f). Together, our data indicate that LAIR1 plays an essential role in development of certain AML and ALL.

LAIR1 deficiency exhausts mouse AML stem cells

Further analysis of the mouse leukemia models enabled a deeper mechanistic investigation of the function of LAIR1. There were significantly more differentiated $B220^+$ and $CD3^+$ cells in secondarily transplanted mice that received *lair1*-null cells than in those given control WT cells (Fig. 4A-D). These differentiated hematopoietic cells increased in numbers from day 18 to day 28 post-transplantation (Supplementary Fig. 4g-i).

The gradual disappearance of *lair1*-null AML after secondary transplantation suggests that LAIR1 supports the activity of AML stem cells (AML-SCs). AML-SCs are enriched in $YFP^+Mac\text{-}1^+Kit^+$ cells in the MLL-AF9-IRES-YFP model [33]. There were approximately 90% fewer $YFP^+Mac\text{-}1^+Kit^+$ *lair1*-null cells at 18 days post-transplantation than in BM of mice transplanted with control AML cells during the secondary transplantation (Fig. 4B; 38% control vs. 4% null). Because AML-SCs have not yet been purified to homogeneity, we further relied on functional measures to evaluate the activity of leukemia stem cells using serial colony forming units (CFU) replating and serial transplantation assays. The *lair1*-null AML cells had an approximately 30% and 90% decrease in CFU upon secondary and tertiary plating respectively (Fig. 4E). The WT $YFP^+Mac\text{-}1^+Kit^+$ AML cells from the secondary transplanted mice formed large, compact colonies, whereas *lair1*-null cells tended to form smaller and more diffuse colonies indicating decreased potency and higher differentiation potential (Fig. 4F). Similarly, when we isolated WT and *lair1*-null $YFP^+Mac\text{-}1^+Kit^+$ cells from the secondarily transplanted mice for the tertiary transplantation, all mice that received the *lair1*-null AML-SCs survived, whereas those transplanted with WT AML-SCs died within 40 days (Fig. 4G). Concordant with observation of human cells treated with *lair1*-targeting shRNA, deletion of *lair1* did not significantly change cell cycle status but dramatically increased both early and late apoptosis in AML cells in the secondarily transplanted mice (Fig. 4H).

To quantitate how LAIR deficiency affects the AML-SC frequency, we performed transplantations with limiting dilutions of sorted YFP^+ WT and *lair1*-null MLL-AF9 BM cells that were collected from primary recipients. Leukemia development, as measured by survival ratio and latency days, is summarized in Fig. 4I. Strikingly, the frequency of functional AML-SCs in *lair1*-null primary MLL-AF9 AML model mice was only 1/53 (= 116/6109) of that in control WT AML mice. Together, our results indicate that LAIR1 sustains the stemness of AML cells.

SHP-1 signaling is essential for the long-term survival of AML stem cells

Because LAIR1 recruits tyrosine phosphatase SHP-1 and SHP-2 for downstream signaling, we sought to determine whether SHP-1 and SHP-2 mediate LAIR1 activity in AML-SCs. Although there was no significant change of total or phospho-SHP-2 levels in WT or *lair1*-null AML cells, both total and phospho-SHP-1 levels were significantly decreased in *lair1*-null AML cells, especially in those samples collected from the secondary transplantation (Fig. 5A).

We introduced retroviruses encoding *shp-1* or *shp-2* into *lair1*-null AML cells that were collected from previously transplanted mice in rescue experiments to determine which

phosphatase mediates the effects of LAIR1 in AML-SCs. The ectopic expression of SHP-1, but not SHP-2, was capable of rescuing the defective phenotype of *lair1*-null AML cells in CFU assays and in transplantation (Fig. 5B-D, Supplementary Fig. 6a).

Furthermore, in the MLL-AF9 model, when SHP-1 was conditionally deleted from leukemia cells by Cre-mediate recombination, the colony-forming ability and the engraftment of leukemia cells into the mice greatly decreased and mice survived significantly longer (Fig. 5E-G). In agreement with the previous finding that SHP-1 is a negative regulator for normal hematopoietic progenitors [37-39], *shp-1* deletion increased normal myeloid CFUs (Fig. 5H, Supplementary Fig. 6b). In addition, in contrast to a decreased SHP-1 protein expression in *lair1*-null bone marrow AML cells, we found that the SHP-1 protein levels in BM cells of WT and *lair1*-null mice were similar as determined by western blotting (Fig. 5I). Collectively, our results indicate that SHP-1 is a negative regulator in normal myeloid progenitors but acts as a key positive signaling mediator of LAIR1 in AML-SCs and prevents exhaustion of AML-SCs.

SHP-1 as an adaptor to recruit CAMK1 in LAIR1-mediated signaling

To further confirm the role of SHP-1 in LAIR1-mediated signaling, we treated mouse and human AML cells with several protein tyrosine phosphatase (PTPase) inhibitors, sodium stibogluconate, NSC-87877, and PHPS1. To our surprise, the treatment did not significantly suppress AML growth (Supplementary Fig. 6c-d). Based on this unexpected finding, we compared the rescue effects of WT SHP-1 with the PTPase-inactive SHP-1 ($C_{453}S$) [40], a tyrosine-mutant SHP-1 4YF (Grb2-binding-independent mutant [41]), or the C-terminal PTPase domain only (PTPc) SHP-1 on *lair1*-null AML cells. Like WT SHP-1, the PTPase-defective SHP-1 and the Grb2-binding-independent SHP-1 rescued the *lair1*-null phenotype. In contrast, the truncated form of SHP-1 containing only the PTPase domain failed to rescue (Fig. 6A-C, Supplementary Fig. 6e). These assays indicated the role of SHP-1 in LAIR1 signaling is independent of its phosphatase activity.

To identify potential downstream effectors of LAIR1 and SHP-1 in AML cells, we sought to identify signaling pathways that are defective in *lair1*-null AML cells. We found no apparent differences in the CAMK1 expression in normal BM samples of WT and *lair1*-null mice (Fig. 5I); however, the total protein level of CAMK1 was decreased in the *lair1*-null AML cells (Fig. 6D). This result is accordant with our previous finding that CAMKs are induced by LILRB2, another ITIM-containing receptor that can also recruits SHP-1/SHP-2 [25]. We thus hypothesized that CAMK1 is a component of LAIR1/SHP-1 signaling. To test this hypothesis, we introduced retroviruses encoding CAMK1 into WT and *lair1*-null defective AML cells. Although ectopic expression of CAMK1 did not affect WT AML cell function, it did functionally rescue the defective phenotype of *lair1*-null AML cells (Fig. 6E-G, Supplementary Fig. 6f).

To test the relationship of LAIR1, SHP-1, and CAMK1, we performed co-immunoprecipitation assays using mouse MLL-AF9 AML cells. The bidirectional pull-down experiments showed that the endogenous SHP-1 and CAMK1 interact with each other (Fig. 6H). We also confirmed that LAIR1 interacted with SHP-1 (Supplementary Fig. 6g), concordant with a previous result [42]. These results suggest that LAIR1/SHP-1/CAMK1 form

a complex in primary AML cells. Importantly, the phosphatase-inactive SHP-1 $C_{453}S$ mutant bound CAMK1, but the phosphatase domain of SHP-1 alone failed to bind to CAMK1 (Fig. 6I). Our data support the conclusion that SHP-1 plays a phosphatase-independent role as an adapter to recruit CAMK1 during LAIR1-mediated signaling in AML cells.

CREB is necessary for LAIR1-mediated signaling

The AML oncogene cAMP response element-binding protein (CREB) [43] is a downstream transcription factor induced by CAMKs [44]. We sought to test whether CREB is a part of the LAIR1/SHP-1/CAMK1 signaling pathway. Phosphorylation of CREB was abundant in WT but not *lair1*-null AML cells (Fig. 7A). WT CREB robustly rescued the defective phenotype of *lair1*-null AML cells *in vitro* and *in vivo*; however none of the mutant CREB (transactivation mutants S129A, S133A, or double mutant S129/133A) [43, 45] had effects on the phenotype of *lair1*-null AML cells (Fig. 7B-D, Supplementary Fig. 7a). A CREB inhibitor XX15 [46, 47] (a derivative of naphthol AS-E [47]) significantly reduced the colony-forming ability of AML cells (Fig. 7E). The transactivation-inactive CREB resulted in decreased SHP-1 levels in AML mice *in vivo* (Supplementary Fig. 6d), suggesting that the lower CREB activation decreases the feedback loop involving SHP-1. Overall, these experiments indicate that CREB is a transcription factor downstream of LAIR1/SHP-1/CAMK1 signaling in AML cells.

LAIR1/SHP-1/CAMK1/CREB signaling is critical for certain human AML development

Our *in silico* analysis indicated that *lair1* was expressed at significantly higher levels by primary human AML BM and PB mononuclear cells than by normal counterparts, and its level negatively correlates with the overall survival of human AML patients (Fig. 8A). Normal human hematopoietic cells contain both $LAIR1^+$ and $LAIR^-$ compartments (Fig. 8B, cord blood); however, 86% of primary human AML specimens contained mostly $LAIR1^+$ cells (Fig. 8B, AML type 2), and only 14% of AML samples had significant populations of both $LAIR1^+$ and $LAIR^-$ cells (Fig. 8B, AML type 1). The separation of $LAIR1^+$ and $LAIR1^-$ leukemia cells followed by CFU assay demonstrated that $LAIR1^+$ AML cells had a significantly higher ability than $LAIR1^-$ AML cells to form colonies in both primary and secondary plating (Supplementary Fig. 8a, bars B1 and B2). By contrast, there was no significant difference in colony-forming potential between the $LAIR^+$ and $LAIR1^-$ populations of human cord blood mononuclear cells (Supplementary Fig. 8a, bar A). More importantly, when AML cells with high LAIR1 expression ($LAIR1^{high}$) or those with low LAIR1 expression ($LAIR1^{low}$) were transplanted into NSG mice, only leukemia cells that expressed significant LAIR1 were able to engraft (Fig. 8C). These data suggest that $LAIR1^+$ cells are enriched for AML-SC activity. Of note, LAIR1 expression is independent of the analyzed phenotypic markers of human AML-SCs (Supplementary Fig. 8e). The LAIR1 knockdown in primary human AML leukemia patient samples significantly inhibited the leukemia development as determined by CFU assays and NSG xenograft experiments (Supplementary Fig. 8f-g). These results suggest that LAIR1 is expressed on human AML-SCs and essential for their growth.

Our *in silico* analysis demonstrated that higher levels of *shp-1* expression significantly correlated with a reduced survival rate for AML patients (Fig. 8D). The knockdown of *shp-1* expression in human MV4-11 cells significantly inhibited cell growth compared to controls (Fig. 8E-F, Supplementary Fig. 8b). These results are consistent with the reported loss-of-function roles of SHP-1 in human leukemia cells [48, 49].

As observed for *shp-1*, the *in silico* analysis indicates that higher levels of *camk1* expression correlated with a decreased survival of AML patients (Fig. 8G). The knockdown of *camk1* in human MV4-11 cells also inhibited cell growth by inducing apoptosis (Fig. 8H-I, Supplementary Fig. 8d). Consistent with the data from *lair1*-null AML cells (Fig. 5A, Fig. 6D), the protein levels of both SHP-1 and CAMK1 decreased in *lair1*-deficient human leukemia cells (Fig. 8J), further supporting our finding that SHP-1 and CAMK1 play important roles in LAIR1 signaling. The *in silico* analysis also indicated that levels of *lair1*, *shp-1*, and *camk1* in AML patients are positively correlated (Fig. 8K). In cells treated with the CREB inhibitor XX15 [46, 47], leukemia cell colony-forming ability was reduced and apoptosis was induced (Fig. 8L-M, Supplementary Fig. 7b-c).

Together, our data suggest LAIR1/SHP-1/CAMK1 work as a complex in AML cells. LAIR1 recruits SHP-1, which serves as an adaptor for CAMK1 activation. CAMK1 activation further induces CREB transactivation. This signaling inhibits apoptosis and differentiation and supports self-renewal of AML-SCs (Supplementary Fig. 8h).

Discussion

Effective elimination of all cancer cells, including cancer stem cells, remains a major challenge in oncology. Our finding that a representative ITIM-receptor LAIR1 supports the survival and self-renewal of leukemia cells identified a potential angle to combat hematopoietic malignancies. We showed that the expression of many known ITIM-receptors inversely correlates with the overall survival of AML patients and that certain of these receptors are crucial for the growth of human acute leukemia cells. We conducted a detailed investigation of LAIR1, which does not affect normal hematopoiesis but is essential for acute leukemia development. Deletion of *lair1* from either mouse or human AML cells induced apoptosis, inhibited growth, and abrogated AML development in transplantation models. Importantly, our data indicate that SHP-1, but not SHP-2, mediates LAIR1 signaling in AML cells and prevents exhaustion of AML-SCs *in vivo*. Furthermore, we demonstrated that, while SHP-1 is a negative signaling molecule for normal myeloid differentiation, SHP-1 acts as a phosphatase-independent adaptor to recruit CAMK1 for activation of the downstream transcription factor CREB in AML cells. The LAIR1/SHP-1/CAMK1 axis may represent a target for treating AML.

The tumor-supportive role of SHP-1 explains why some immune inhibitory receptors such as LAIR1 directly support cancer development. SHP-1 is capable of binding to Grb2 in a phosphatase-independent manner [41]; however, the CAMK1 recruitment by SHP-1 represents a different phosphatase-independent mechanism. A role for SHP-1 in AML development is also supported by evidence from other studies showing that SHP-1 suppresses differentiation [48] and inhibits apoptosis in some leukemia cells [49]. Nevertheless, it is

possible that SHP-1 inhibits the growth of certain tumors and certain immortalized cell lines other than the ones we studied here. Moreover, the signaling through LAIR1 observed in leukemia cells unlikely exists in normal cells. In contrast to the role of SHP-1 as an adaptor or scaffolding protein in AML development, the phosphatase activity of SHP-1 is necessary in normal hematopoietic functions. For example, the myeloproliferative phenotype of me^v/me^v mice is caused by inactivation of the phosphatase activity of SHP-1 [38, 50]. In addition, although the LAIR1 deficiency greatly reduced the level of SHP-1 and CAMK1 in leukemia samples, these protein levels were not affected by *lair1*-deficiency in normal bone marrow cells (Fig. 5I).

Although CAMK1 is predominantly cytoplasmic [51], it can be transported into the nucleus with the existence of a nuclear translocation sequence [52]. Therefore, the activation of CREB by CAMK1 is possibly direct. Additional downstream targets of CAMK1 other than CREB likely also exist. We speculate that LAIR1/SHP-1/CAMK1 may form a complex that is necessary for the activation or even stability of SHP-1 and CAMK1. A LAIR1 deficiency may initially result in somewhat decreased activation of SHP-1, CAMK1, and CREB. This decrease should become more severe over time (compare our SHP-1 levels in primary and secondarily transplanted AML mice in Fig. 5A) because of a possible feedback loop involving CREB and SHP-1: Less activation of CREB will lead to more decreased SHP-1 over time in *lair1*-null AML cells, eventually resulting in the exhaustion of the signaling system (Supplementary Fig 7d).

The supportive role of LAIR1 in AML is unlikely to be an exceptional case in cancer biology. As we showed, the *lair1* deficiency has a similar effect to the B-ALL model, suggesting LAIR1 also supports certain ALL. In addition, our study suggests that a number of other ITIM-receptors support AML development, and thus may also activate a similar downstream signaling pathway as LAIR1 in AML cells. Because there are numerous types of ITIM-receptors, different receptors may have different expression patterns in different types or subtypes of leukemia and other cancers. It will be important to investigate the mechanisms by which other ITIM-receptors support cancer progression.

The identification of ITIM-receptors and their downstream signaling as potential therapeutic targets may reshape our views regarding how leukemia develops, how cancer cells differ from other cells, and how to treat this difficult disease. Our study suggests that some leukemia cells have unique signaling pathways downstream of ITIM- receptors. These inhibitory receptors may enable the leukemia cells to survive conventional therapies, resulting in tumor relapse. Because inhibition of the signaling of certain ITIM-receptors directly blocks leukemia growth, and stimulates immunity [26, 27] that may suppress tumorigenesis but does not disturb normal hematopoiesis [29], these ITIM-receptors represent ideal targets for treating leukemia. The blockade of inhibitory receptor signaling in combination with conventional therapies may prove to be an effective strategy for elimination of leukemia cells. It will be interesting to test whether therapeutic modalities for ITIM-receptors may include antibodies against the extracellular domains of these receptors or whether inhibition of the intracellular signaling of ITIM-receptors will represent a more powerful means of blocking these targets.

Methods

Mice

C57 BL/6 CD45.2, CD45.1, and NSG mice were purchased from the National Cancer Institute and from the University of Texas Southwestern Medical Center animal breeding core facility. *lair1*-null mice were previously described [29]. Mice were maintained at the University of Texas Southwestern Medical Center animal facility. No statistical method was used to predetermine sample size. The experiments were not randomized. The investigators were not blinded to allocation of animals during experiments and outcome assessment. All animal experiments were performed with the approval of UT Southwestern Committee on Animal Care.

Human leukemia cells

Primary human AML samples were obtained from the tissue bank at the University of Texas MD Anderson Cancer Center. Informed consent was obtained under a protocol reviewed and approved by the Institutional Review Board at the University of Texas MD Anderson Cancer Center. Samples were frozen in fetal bovine serum (FBS) with 10% DMSO and stored in liquid nitrogen. Human leukemia cell lines were cultured in RPMI supplemented with 10% FBS at 37 °C in 5% CO_2 and the normal level of O_2. Human leukemia cell lines were from ATCC.

TCGA analyses

Data were obtained from the TCGA AML database (https://tcga-data.nci.nih.gov/tcga/; accessed November 5, 2012), and levels were normalized to *GADPH* expression, unless indicated. Patients were separated into two groups based on whether they had higher (n = 82 patient samples) or lower (n = 83 patient samples), with the exception for *lair1* analysis in which n= 52 patient samples were used for these two groups. For correlation analysis, scatter plots with regression curve (blue) and 95% prediction interval (red) indicate the positive correlations among CAMKI, LAIR1 or PTPN6. Correlation coefficient r and p-value were shown in Fig. 8K.

Chimeric receptor reporter cells

We constructed a stable chimeric receptor reporter cell system to test the ability of a ligand to bind to the extracellular domain (ECD) of LAIR1 and trigger the activation or inhibition of the chimerically fused intracellular domain of paired immunoglobulin-like receptor β, which signals through the adaptor DAP-12 to activate the NFAT promoter. If an agonist or antagonist binds the ECD and activates or suppresses the chimeric signaling domain, we will observe an increase or decrease, respectively, of GFP expression driven by the NFAT promoter. This reporter system serves as a sensitive surrogate that enables us to study the signaling-induction and inhibition abilities of ligands.

Flow cytometry

For flow cytometry analyses of mouse AML cells, peripheral blood or BM cells were stained with anti-Mac-1-APC (rat, M1/70, 1:200 dilution), anti-Gr-1-PE (rat, RB6-8C5,

1:200 dilution), anti-CD3-APC (hamster, 145-2C11, 1:200 dilution), anti-B220-PE (rat, RA3-6B2, 1:200 dilution), or anti-Kit-PE (rat, 2B8, 1:200 dilution) monoclonal antibodies (BD Pharmingen). For analysis of apoptosis, GFP or YFP positive AML cells were stained at indicated days with PE-conjugated anti-Annexin V and 7-AAD (BD Pharmingen) according to the manufacturer's instructions. For analysis of human hematopoietic engraftment in NSG mice, we followed our previously published protocol [53, 54] and used anti-human LAIR1 (clone 342219, R&D Systems) and anti-human CD45-PE (mouse, HI30, BD Pharmingen, 1:50 dilution) to quantify the total human AML engraftment.

Cell growth assay

RFP^+ or GFP^+ cells were sorted by flow cytometry one day post-infection and 20,000 cells were plated in 1.55-cm wells. Cell numbers were determined on days 2, 4, and 6 in triplicate wells. The experiment was repeated three times with similar results.

Mouse competitive reconstitution analyses

The indicated numbers of mouse CD45.2 donor cells were mixed with 1×10^5 freshly isolated CD45.1 competitor BM cells and the mixture was injected intravenously via the retro-orbital route into 6-8 week old CD45.1 mice previously irradiated with a total dose of 10 Gy. For secondary transplantation, $1{\times}10^6$ BM cells from primary transplanted mice were transplanted into mice with $2{\times}10^5$ normal BM cells as competitors. To measure reconstitution, peripheral blood was collected at the indicated time points post-transplantation, and the presence of $CD45.1^+$ and $CD45.2^+$ cells in lymphoid and myeloid compartments were measured as described [54, 55].

Human AML xenograft

Xenografts were performed essentially as we described [53, 54]. Briefly, adult NSG mice (6–8 weeks old) were sub-lethally irradiated with 250 cGy total body irradiation prior to transplantation. shRNA-infected cells were resuspended in 200 μl PBS containing 1% FBS at a final concentration of $0.5 - 1 \times 10^6$ human $CD45^+$ viable cells per mouse for retro-orbital injection. One to four months after transplantation, the PB, BM, spleen, and liver were assessed for the engraftment.

Selection of a specific shRNA targeting *lari1*

To exclude the possibility of off-target effects of the shRNAs, we constructed a *lari1* transgene with the shRNA-226 target sequence mutated. Six mutations (-AA GC***A*** AG***C*** CC***T*** TC***A*** GA***A*** TC***T*** G-) were introduced (as indicated by italicized letters in the region of *lair1* targeted by shRNA) into the *lair1* WT plasmid to create Flag-*lair1*-6m or RFP-*lair1*-6m. We infected MV4-11 cells with this mutant (6m) or wild-type (WT) *lair1*-encoding lentiviruses. Upon treatment of these cells with shRNA-226, the cells infected with WT *lair1* failed to grow, whereas the cells infected with the mutant proliferated (Fig. 1F-G). This result indicates that shRNA-226 specifically targeted *lair1* mRNA and that the cell growth block resulted from *lair1* silencing. shRNA-226 was used in subsequent experiments to specifically inhibit expression of *lair1*.

Virus construction/infection and AML transplantation

The lentiviral vector Pll3.7 was used to express shRNAs designed to target *lair1*, *shp-1*, and other ITIM-containing receptor mRNAs (sequences listed in suppl. Table 2). Lentiviral vector ZsRed was used to construct WT lair1and 6mut lair1. The mutations were introduced by using the QuickChange Mutagenesis kit (Stratagene). For virus packaging, retroviral constructs MSCV-MLL-AF9-IRES-YFP, MSCV-SHP-1-IRES-GFP, MSCV-SHP-1 C453S-IRES-GFP, MSCV-SHP-1 4YF-IRES-GFP, MSCV-SHP-1 PTPc-IRES-GFP, MSCV-CAMK1-IRES-GFP, MSCV-CREB-IRES-GFP, MSCV-CREB S129A-IRES-GFP, MSCV-CREB S133A-IRES-GFP, MSCV-CREB S129/133A-IRES-GFP MSCV-SHP-2-IRES-GFP, Mig-Cre, Mig-AML1-ETO9a, or PMXS-Ig-N-Myc, were mixed with PCL-ECO (2:1), and the lentivirus constructs were mixed with pSPAX2 and pMD2.G (4:3:1), followed by transfection into 293T cells using Lipofectamine 2000 (Invitrogen). Virus-containing supernatant was collected 48-72 hours post-transfection and used for infection as described previously [56]. Infected mouse Lin^- cells (300,000) or human cells (indicated numbers) were transplanted into lethally irradiated (1,000 rad) C57BL/6 mice (6–8 weeks old) or sublethally irradiated (250 rad) NSG mice by retro-orbital injection. For the 2nd and tertiary transplantation, we used FACS to isolate YFP^+ BM cells from primary and secondary recipient mice respectively and transplanted 3000 cells into lethally irradiated recipients. We conducted 7 independent secondary transplantation experiments from 2 batches of the primary MLL-AF9 leukemia samples. In the first two independent experiments, we used one primary sample and obtained very similar results. We then performed an additional 5 experiments, by pooling 3 samples for transplantation for a total of 5 times and also obtained similar results.

Leukemia characterization

In the retrovirus transplantation model, we isolated Lin^- cells from littermate *lair1*-null and WT mice, infected them with MSCV-oncogene-IRES-YFP retrovirus followed by transplantation into WT recipient mice to establish leukemic mice. We monitored the survival, examined the size and histological properties of BM, spleen, and liver, and analyzed the numbers and infiltration of leukemia cells in PB, BM, spleen, and liver. We also determined the different populations of leukemia cells using flow cytometry. Serial CFU replating, serial transplantation, and limiting dilution assays were performed as indicated.

In vitro and *in vivo* rescue assays in mouse leukemia model study

MLL-$AF9^+$ WT or *lair1*-null BM cells in secondarily transplanted mice were harvested at 28 days and were infected with individual interested gene encoding or control viruses. Mutant genes were expressed at levels similar to that of WT. C57BL/6 mice (6–8 weeks old) were transplanted with 3,000 of these ectopically gene-expressing or control AML cells for survival curve analysis. Percentages of retrovirus-infected (GFP^+) AML cells in PB of recipient mice after 28 days of transplantation (n = 5 mice) were measured. For in vitro CFU assay, 2000 of ectopically gene-expressing or control AML cells were plated, and 5 days later the CFU number were calculated. The secondary and tertiary platings were performed by harvesting and sorting the GFP^+ primary CFU cells.

Southern blotting

Genomic DNA was extracted from spleens using the Gentra Systems kit (Gentra Systems, Minneapolis, MN, USA). For Southern analyses, 10 μg genomic DNA was digested with EcoRI (New England Biolabs, USA) overnight at 37 °C and run on a 1% agarose gel. DNA was transferred overnight to a Genescreen Plus nylon membrane (Perkin Elmer, Boston, MA, USA). Membranes were probed with 10^6 CPM per ml of [α32P] dCTP (Perkin Elmer)-labeled yellow fluorescent protein (YFP). The YFP probe was derived from the 508bp fragment of the MLL-AF9-IRES-YFP vector, and was radiolabeled by PCR.

Colony assays

Human or mouse AML cells were diluted to the indicated concentration in IMDM with 2% FBS and were then seeded into methylcellulose medium H4436 or M3534 (StemCell Technologies) for myeloid colony formation analysis as described previously [55].

Western blotting

Cell lysates (100 μg samples) were prepared by Transmembrane Protein Extraction Reagent (FIVEphoton Biochemicals, TmPER-200) or RIPA buffer, and were separated by electrophoresis on 4-15% SDS-polyacrylamide gels, and the proteins were electroblotted onto a nitrocellulose membrane. The membrane was probed with indicated primary antibody for 1 h at room temperature and then incubated with horseradish peroxidase-conjugated secondary antibody, which was detected with the Luminata Crescendo Western HRP Substrate (Millipore). The antibody used in this paper included: surfactant protein D (ab17781), SHP-1 (ab2020, 1:2000 dilution), CAMK1 (ab68234, 1:2000 dilution), mLAIR1 (ab171239, 1:500 dilution), CAMKIV (ab3557, 1:4000 dilution), CREB (ab5803, 1:2000 dilution), p-SHP-1 (Y536, ab51171, 1:1000 dilution) from Abcam; SHP-2 (3397s, 1:1000 dilution), p-SHP2 (Tyr580, 3703, 1:1000 dilution), p-CREB (S133, 9198, 1:2000 dilution) from cell signaling; anti-Flag M2 (F1804, sigma, 1:10000 dilution), actin (A5228, 1:10000 dilution) and human LAIR1 (LS-C44463, lifespan biosciences, 1:2000 dilution). A representative image was shown from at least 3 similar images.

Statistical analyses

Data are expressed as mean ± SEM. Data were analyzed by Student's t test and were considered statistically significant if $p < 0.05$. The survival rates of the two groups were analyzed using a log-rank test and were considered statistically significant if $p < 0.05$. p values are represented as precise values or as *** $p < 0.0001$.

Supplementary Material

Refer to Web version on PubMed Central for supplementary material.

Acknowledgments

We would like to thank Dr. Hideyuki Saya from Keio University School of Medicine for the pMX-IG N-Myc vector. We appreciate the support of staff of the tissue bank at the Department of Hematopathology, the University of Texas MD Anderson Cancer Center. Support to C.C.Z. was from NIH grant 1R01CA172268, Leukemia & Lymphoma Society Awards 1024-14 and TRP-6024-14, CPRIT RP140402, and When Everyone Survives Foundation. J.W.T. is supported by grants from the V Foundation for Cancer Research, the William Lawrence and

Blanche Hughes Fund, and the National Cancer Institute (4 R00CA151457-03), and the Leukemia & Lymphoma Society. X. X. is supported by Susan G. Komen Foundation and RO1GM087305. J.E.C. is supported by the intramural program of the National Institute of Allergy and Infectious Diseases. M.J.Y. is supported in part by NIH/NCI R01 CA164346, Ladies Leukemia League, Developmental Research Awards in Leukemia SPORE CA100632, and Center for Inflammation and Cancer, IRG, Center for Genetics and Genomics, Sister Institution Network Fund and Physician Scientist Award of the University of Texas MD Anderson Cancer Center.

References

1. Maynadie M, et al. Twenty-five years of epidemiological recording on myeloid malignancies: data from the specialized registry of hematologic malignancies of Cote d'Or (Burgundy, France). Haematologica. 2011; 96:55–61. [PubMed: 20971817]
2. Krause DS, Van Etten RA. Right on target: eradicating leukemic stem cells. Trends Mol Med. 2007; 13:470–481. [PubMed: 17981087]
3. Lapidot T, et al. A cell initiating human acute myeloid leukaemia after transplantation into SCID mice. Nature. 1994; 367:645–648. [PubMed: 7509044]
4. Lane SW, Scadden DT, Gilliland DG. The leukemic stem cell niche: current concepts and therapeutic opportunities. Blood. 2009; 114:1150–1157. [PubMed: 19401558]
5. Wei J, et al. Microenvironment determines lineage fate in a human model of MLL-AF9 leukemia. Cancer Cell. 2008; 13:483–495. [PubMed: 18538732]
6. Ishikawa F, et al. Chemotherapy-resistant human AML stem cells home to and engraft within the bone-marrow endosteal region. Nat Biotechnol. 2007; 25:1315–1321. [PubMed: 17952057]
7. Imbesi S, et al. Oxidative stress in oncohematologic diseases: an update. Expert Rev Hematol. 2013; 6:317–325. [PubMed: 23782085]
8. Fathi A, Levis M. FLT3 inhibitors: a story of the old and the new. Curr Opin Hematol. 2011; 18:71–76. [PubMed: 21245757]
9. Vainchenker W, Constantinescu SN. JAK/STAT signaling in hematological malignancies. Oncogene. 2013; 32:2601–2613. [PubMed: 22869151]
10. Broxmeyer HE. Chemokines in hematopoiesis. Curr Opin Hematol. 2008; 15:49–58. [PubMed: 18043246]
11. Jin L, Hope KJ, Zhai Q, Smadja-Joffe F, Dick JE. Targeting of CD44 eradicates human acute myeloid leukemic stem cells. Nat Med. 2006; 12:1167–1174. [PubMed: 16998484]
12. Krause DS, Lazarides K, von Andrian UH, Van Etten RA. Requirement for CD44 in homing and engraftment of BCR-ABL-expressing leukemic stem cells. Nat Med. 2006; 12:1175–1180. [PubMed: 16998483]
13. Miller PG, et al. In Vivo RNAi screening identifies a leukemia-specific dependence on integrin beta 3 signaling. Cancer Cell. 2013; 24:45–58. [PubMed: 23770013]
14. Chao MP, et al. Anti-CD47 antibody synergizes with rituximab to promote phagocytosis and eradicate non-Hodgkin lymphoma. Cell. 2010; 142:699–713. [PubMed: 20813259]
15. Jan M, et al. Prospective separation of normal and leukemic stem cells based on differential expression of TIM3, a human acute myeloid leukemia stem cell marker. Proc Natl Acad Sci U S A. 2011; 108:5009–5014. [PubMed: 21383193]
16. Horton SJ, Huntly BJ. Recent advances in acute myeloid leukemia stem cell biology. Haematologica. 2012; 97:966–974. [PubMed: 22511496]
17. Weng AP, et al. Activating mutations of NOTCH1 in human T cell acute lymphoblastic leukemia. Science. 2004; 306:269–271. [PubMed: 15472075]
18. Zhao C, et al. Loss of beta-Catenin Impairs the Renewal of Normal and CML Stem Cells In Vivo. Cancer Cell. 2007; 12:528–541. [PubMed: 18068630]
19. Wang Y, et al. The Wnt/beta-catenin pathway is required for the development of leukemia stem cells in AML. Science. 2010; 327:1650–1653. [PubMed: 20339075]
20. Zhao C, et al. Hedgehog signalling is essential for maintenance of cancer stem cells in myeloid leukaemia. Nature. 2009; 458:776–779. [PubMed: 19169242]
21. Krause DS, et al. Differential regulation of myeloid leukemias by the bone marrow microenvironment. Nat Med. 2013; 19:1513–1517. [PubMed: 24162813]

22. Heidel FH, Mar BG, Armstrong SA. Self-renewal related signaling in myeloid leukemia stem cells. Int J Hematol. 2011; 94:109–117. [PubMed: 21800073]
23. Konopleva MY, Jordan CT. Leukemia stem cells and microenvironment: biology and therapeutic targeting. J Clin Oncol. 2011; 29:591–599. [PubMed: 21220598]
24. Sands WA, Copland M, Wheadon H. Targeting self-renewal pathways in myeloid malignancies. Cell Commun Signal. 2013; 11:33. [PubMed: 23675967]
25. Zheng J, et al. Inhibitory receptors bind Angptls and support blood stem cells and leukemia development. Nature. 2012; 485:656–660. [PubMed: 22660330]
26. Takai T, Nakamura A, Endo S. Role of PIR-B in autoimmune glomerulonephritis. J Biomed Biotechnol. 2011; 2011:275302. [PubMed: 20976309]
27. Daeron M, Jaeger S, Du Pasquier L, Vivier E. Immunoreceptor tyrosine-based inhibition motifs: a quest in the past and future. Immunol Rev. 2008; 224:11–43. [PubMed: 18759918]
28. Kim T, et al. Human LilrB2 is a beta-amyloid receptor and its murine homolog PirB regulates synaptic plasticity in an Alzheimer's model. Science. 2013; 341:1399–1404. [PubMed: 24052308]
29. Tang X, et al. Leukocyte-associated Ig-like receptor-1-deficient mice have an altered immune cell phenotype. J Immunol. 2012; 188:548–558. [PubMed: 22156345]
30. Olde Nordkamp MJ, et al. Leukocyte-associated Ig-like receptor-1 is a novel inhibitory receptor for surfactant protein D. J Leukoc Biol. 2014; 96:105–111. [PubMed: 24585933]
31. Meyaard L. LAIR and collagens in immune regulation. Immunol Lett. 2010; 128:26–28. [PubMed: 19836418]
32. Maasho K, et al. The inhibitory leukocyte-associated Ig-like receptor-1 (LAIR-1) is expressed at high levels by human naive T cells and inhibits TCR mediated activation. Mol Immunol. 2005; 42:1521–1530. [PubMed: 15950745]
33. Krivtsov AV, et al. Transformation from committed progenitor to leukaemia stem cell initiated by MLL-AF9. Nature. 2006; 442:818–822. [PubMed: 16862118]
34. Somervaille TC, Cleary ML. Identification and characterization of leukemia stem cells in murine MLL-AF9 acute myeloid leukemia. Cancer Cell. 2006; 10:257–268. [PubMed: 17045204]
35. Yan M, et al. A previously unidentified alternatively spliced isoform of t(8;21) transcript promotes leukemogenesis. Nat Med. 2006; 12:945–949. [PubMed: 16892037]
36. Sugihara E, et al. Ink4a and Arf are crucial factors in the determination of the cell of origin and the therapeutic sensitivity of Myc-induced mouse lymphoid tumor. Oncogene. 2011
37. Tapley P, et al. Increased G-CSF responsiveness of bone marrow cells from hematopoietic cell phosphatase deficient viable motheaten mice. Exp Hematol. 1997; 25:122–131. [PubMed: 9015212]
38. Paulson RF, Vesely S, Siminovitch KA, Bernstein A. Signalling by the W/Kit receptor tyrosine kinase is negatively regulated in vivo by the protein tyrosine phosphatase Shp1. Nat Genet. 1996; 13:309–315. [PubMed: 8673130]
39. Lorenz U, et al. Genetic analysis reveals cell type-specific regulation of receptor tyrosine kinase c-Kit by the protein tyrosine phosphatase SHP1. J Exp Med. 1996; 184:1111–1126. [PubMed: 9064328]
40. Timms JF, et al. Identification of major binding proteins and substrates for the SH2-containing protein tyrosine phosphatase SHP-1 in macrophages. Mol Cell Biol. 1998; 18:3838–3850. [PubMed: 9632768]
41. Minoo P, Zadeh MM, Rottapel R, Lebrun JJ, Ali S. A novel SHP-1/Grb2-dependent mechanism of negative regulation of cytokine-receptor signaling: contribution of SHP-1 C-terminal tyrosines in cytokine signaling. Blood. 2004; 103:1398–1407. [PubMed: 14551136]
42. Xu M, Zhao R, Zhao ZJ. Identification and characterization of leukocyte-associated Ig-like receptor-1 as a major anchor protein of tyrosine phosphatase SHP-1 in hematopoietic cells. J Biol Chem. 2000; 275:17440–17446. [PubMed: 10764762]
43. Shankar DB, et al. The role of CREB as a proto-oncogene in hematopoiesis and in acute myeloid leukemia. Cancer Cell. 2005; 7:351–362. [PubMed: 15837624]

44. Liu F, Thompson MA, Wagner S, Greenberg ME, Green MR. Activating transcription factor-1 can mediate Ca(2+)- and cAMP-inducible transcriptional activation. J Biol Chem. 1993; 268:6714–6720. [PubMed: 8384217]
45. Tyson DR, Swarthout JT, Jefcoat SC, Partridge NC. PTH induction of transcriptional activity of the cAMP response element-binding protein requires the serine 129 site and glycogen synthase kinase-3 activity, but not casein kinase II sites. Endocrinology. 2002; 143:674–682. [PubMed: 11796524]
46. Xiao, X., Li, B.X. & Xie, F. (ed. O.H.S. University) USA; 2012).
47. Li BX, Xiao X. Discovery of a small-molecule inhibitor of the KIX-KID interaction. Chembiochem. 2009; 10:2721–2724. [PubMed: 19810079]
48. Eklund EA, Goldenberg I, Lu Y, Andrejic J, Kakar R. SHP1 protein-tyrosine phosphatase regulates HoxA10 DNA binding and transcriptional repression activity in undifferentiated myeloid cells. J Biol Chem. 2002; 277:36878–36888. [PubMed: 12145285]
49. Tibaldi E, et al. Lyn-mediated SHP-1 recruitment to CD5 contributes to resistance to apoptosis of B-cell chronic lymphocytic leukemia cells. Leukemia. 2011; 25:1768–1781. [PubMed: 21701493]
50. Shultz LD, et al. Mutations at the murine motheaten locus are within the hematopoietic cell protein-tyrosine phosphatase (Hcph) gene. Cell. 1993; 73:1445–1454. [PubMed: 8324828]
51. Picciotto MR, Zoli M, Bertuzzi G, Nairn AC. Immunochemical localization of calcium/calmodulin-dependent protein kinase I. Synapse. 1995; 20:75–84. [PubMed: 7624832]
52. Stedman DR, Uboha NV, Stedman TT, Nairn AC, Picciotto MR. Cytoplasmic localization of calcium/calmodulin-dependent protein kinase I-alpha depends on a nuclear export signal in its regulatory domain. FEBS Lett. 2004; 566:275–280. [PubMed: 15147908]
53. Zhang CC, Kaba M, Iizuka S, Huynh H, Lodish HF. Angiopoietin-like 5 and IGFBP2 stimulate ex vivo expansion of human cord blood hematopoietic stem cells as assayed by NOD/SCID transplantation. Blood. 2008; 111:3415–3423. [PubMed: 18202223]
54. Zheng J, et al. Ex vivo expanded hematopoietic stem cells overcome the MHC barrier in allogeneic transplantation. Cell Stem Cell. 2011; 9:119–130. [PubMed: 21816363]
55. Huynh H, et al. IGF binding protein 2 supports the survival and cycling of hematopoietic stem cells. Blood. 2011; 118:3236–3243. [PubMed: 21821709]
56. Zheng J, Huynh H, Umikawa M, Silvany R, Zhang CC. Angiopoietin-like protein 3 supports the activity of hematopoietic stem cells in the bone marrow niche. Blood. 2011; 117:470–479. [PubMed: 20959605]

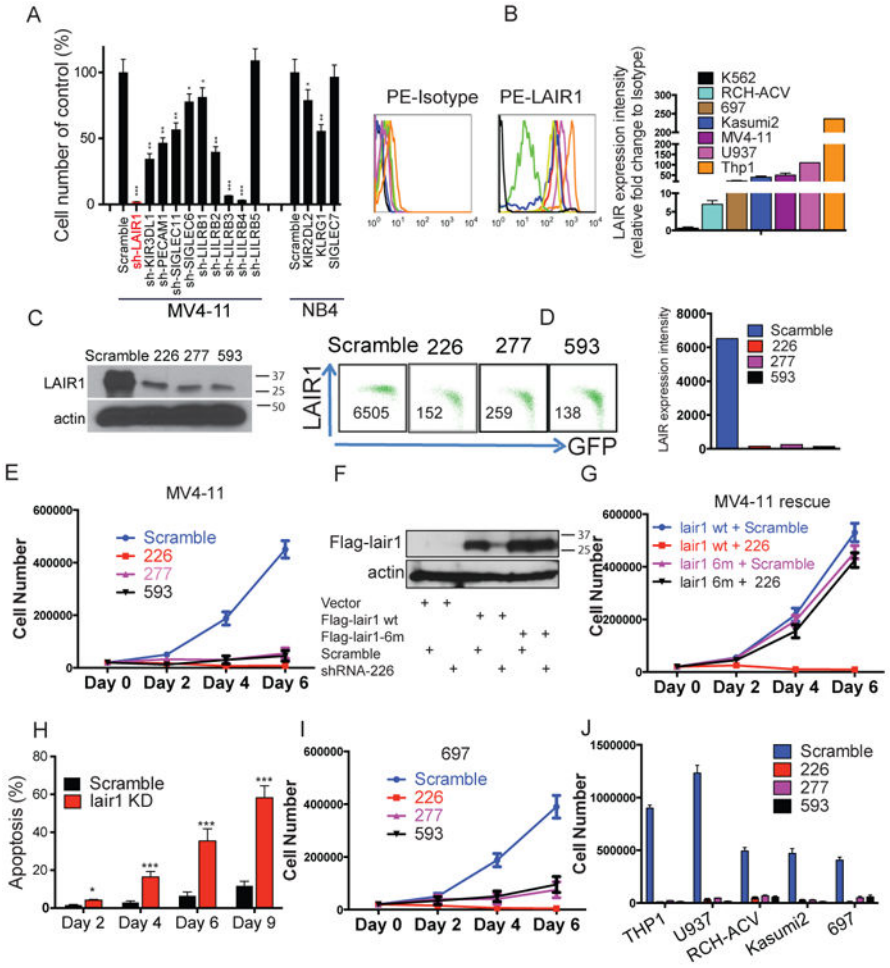

Fig 1. Lair1, a representative ITIM-receptor, is essential for the growth of human leukemia cell lines

A, Effects of shRNA-mediated silencing of expression of indicated ITIM receptors on growth of MV4-11 and NB4 AML cells. The cells were counted on day 6 post-infection, and normalized to cells treated with scrambled shRNAs (mean ± s.e.m., Student's t-test; n=3 samples, sh-LAIR1 *** $p < 0.0001$; sh-KIR3DL1 ** $p = 0.0051$; sh-PECAM1 ** $p = 0.0061$; sh-SIGLEC11 ** $p = 0.0089$; sh-SIGLEC6 * $p = 0.0326$; sh-LILRB1 * $p = 0.0412$; sh-LILRB2 ** p = 00059; sh-LILRB3 *** $p < 0.0001$; sh-LILRB4 *** $p < 0.0001$; sh-KIR2DL2 * $p = 0.0182$; sh-KIRG1 ** $p = 0.0096$).

B, Flow cytometry analysis showing that LAIR1 is highly expressed on the cell surfaces of RCH-ACV, 697, Kasumi2, MV4-11, U937, and THP1 human leukemia cells but not on K562 cells. X-axis indicates LAIR1 expression, and Y-axis indicates cell numbers. The bar graph summarized MFIs of cell surface LAIR1 (relative fold changes to isotype control).

C, Endogenous LAIR1 expression was inhibited by lentivirus vector-based expression of different shRNAs (226, 277, 593) in MV4-11 cells as determined by western blotting at 48 hours after lentiviral infection.

D, Cell-surface LAIR1 expression was inhibited by shRNAs in MV4-11 cells as determined by flow cytometry at 48 hours after lentiviral infection. MFIs (obtained after subtraction of the background MFI of the unstained control) indicate LAIR1 expression levels; GFP

expression indicates infection. Data are from a single experiment, representative of 3 independent experiments.

E, Treatment with shRNA targeting *lair1* inhibited the growth of MV4-11 cells.

F, Expression from Flag-*lair1*-6m is not silenced by shRNA 226 as determined by western blotting.

G, Rescue of *lair1*-knockdown phenotype. RFP-tagged mutant *lair1 (6m)* infected MV4-11 cells are resistant to the shRNA 226-induced growth inhibition.

H, Apoptosis is increased in MV4-11 cells after treatment with shRNA 226 to inhibit *lair1* expression (mean ± s.e.m., Student's t-test; n=3 samples, Day 2 * $p = 0.0112$; Day 4 *** $p < 0.0001$; Day 6 *** $p < 0.0001$; Day 9 *** $p < 0.0001$).

I, Treatment with each shRNA targeting *lair1* inhibited the growth of 697 cells.

J, *Lair1* knockdown inhibited the growth of THP1, U937, RCH-ACV, and Kasumi2 cells as measured on day 6.

In Figs 1B, E, G, I, and J, data from one experiment with n=3 technical replicate samples are shown. The experiment was repeated 3 times with similar results.

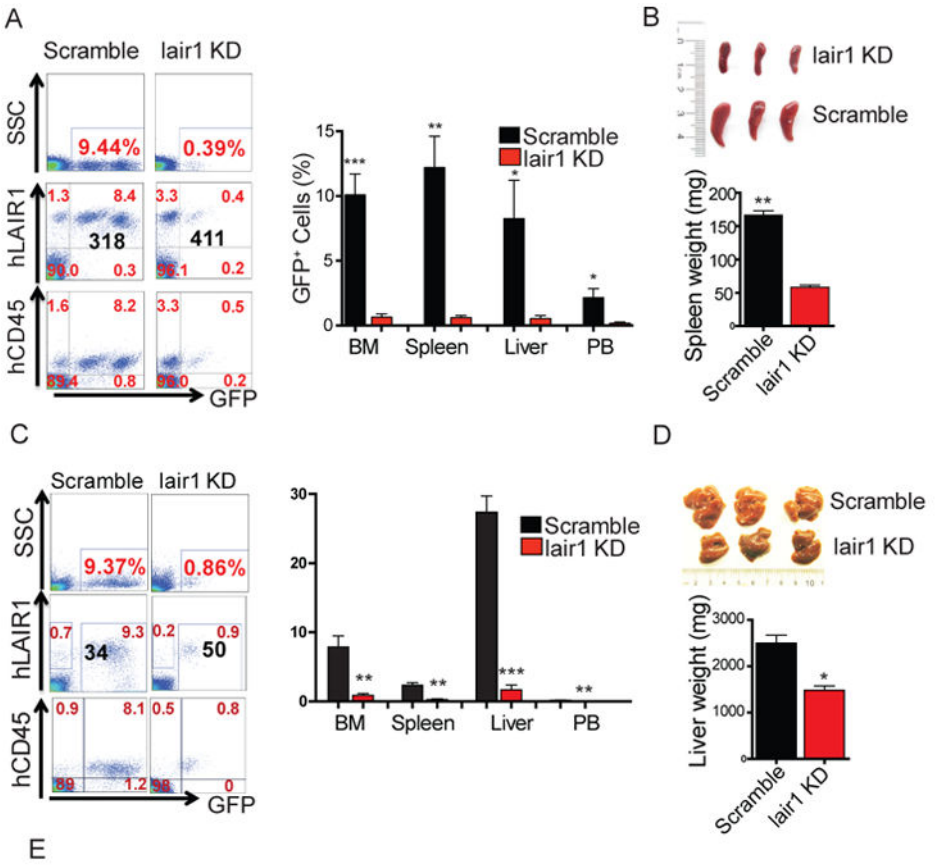

Human leukemia cell lines	MV4-11	THP1	U937	K562	697	RCH-ACV	Kasumi2
Cell growth inhibition	+	+	+	-	+	+	+
Xenograft inhibition	+				+		

Fig 2. Knockdown of *lair1* blocks xenograft of human leukemia cell lines

A, MV4-11 cells (1×10^6 cells) were infected with virus designed to express GFP and either scrambled shRNA or shRNA 226. GFP^+ cells were collected and transplanted into NSG mice (n = 7 mice) one day post-infection. Left panels show representative flow cytometry plots indicating decreased BM engraftment of MV4-11 cells treated with shRNA targeting *lair1*. Staining with anti-human CD45 and anti-LAIR1 antibodies confirmed engraftment was from transplanted human leukemia cells. The percentages of each population are indicated in red numbers, and the median fluorescent intensity of LAIR1 expression is indicated in black numbers. The panel on the right plots percentages of GFP^+ cells in BM, spleen, liver, and PB at 1 month after transplantation (mean ± s.e.m., Student's t-test; n=7 samples, BM *** $p < 0.0001$; Spleen ** $p = 0.0004$; Liver * $p = 0.0233$; PB * $p = 0.01471$).

B, Comparison of the sizes of spleens of the mice transplanted with control MV4-11 leukemia cells or cells expressing shRNA targeting *lair1* (mean ± s.e.m., Student's t-test; n=7 samples, ** $p = 0.0028$).

C, GFP^+ 697 cells infected by scrambled shRNA or shRNA 226 virus were collected, and 5×10^5 cells were transplanted into NSG mice (n = 5 mice for Scramble, n = 7 mice for lair1 null). Left are representative flow cytometry plots showing the decreased BM engraftment of *lair1*-knockdown 697 cells. Human CD45 and LAIR1 antibody staining confirmed

engraftment was from transplanted human leukemia cells. The percentages of each population are indicated in red numbers, and the median fluorescent intensity of LAIR1 expression is indicated in black numbers. Shown on the right are percentages of GFP^+ cells in BM, spleen, liver, and PB at 1 month after transplantation (mean ± s.e.m., Student's t-test; n = 5 mice for Scramble, n = 7 mice for lair1 null, BM ** p = 0.0004; Spleen ** p = 0.0002; Liver *** p <0.0001; PB * p = 0.0057).

D, Comparison of the sizes of livers of the mice transplanted with control or *lair1*-knockdown 697 leukemia cells (mean ± s.e.m., Student's t-test; n = 5 mice for Scramble, n = 7 mice for lair1 null, * p = 0.0048).

E, Summary of the effects of *lair1* silencing in the indicated human leukemia cell lines on inhibition of cell growth *in vitro* and xenograftment in NSG mice.

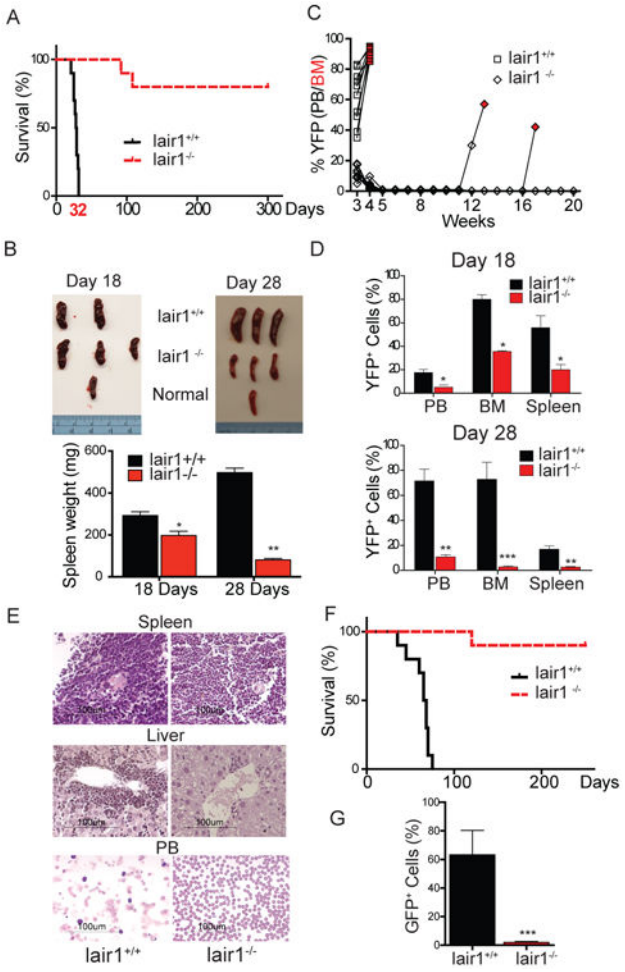

Fig 3. LAIR1 enhances development of MLL-AF9 mouse AML during serial transplantation

A, Survival curves of mice receiving 3,000 pooled YFP$^+$ BM cells that were collected from primary recipients transplanted with WT or *lair1*-null MLL-AF9 AML cells (n = 10 mice; p = 0.00002, log-rank test).

B, Comparison of the spleen sizes of mice that were transplanted with WT or *lair1*-null MLL-AF9 AML cells collected from secondary recipients at 18 days or 28 days after transplantation (mean ± s.e.m., Student's t-test; n = 5 mice, 18 days * p = 0.0245; 28 days ** p = 0.0006).

C, Summary of the percentages of YFP$^+$ WT and *lair1*-null MLL-AF9 leukemia cells in PB (open squares or open diamonds) or BM (red squares or red diamonds) of secondarily transplanted mice over time. Mice that were moribund and euthanized are indicated by red spots, in which the percentages of YFP$^+$ cells in BM (instead of PB) were used in this analysis (n = 10 mice).

D, Summary of percentages of YFP$^+$ AML cells in PB, BM, and spleen of secondary recipient mice transplanted with the WT or *lair1*-null MLL-AF9 AML cells at day 18 (upper panel) and at day 28 (lower panel) post-transplant (mean ± s.e.m., Student's t-test; n = 5 mice, 18 days PB * p = 0.0124; BM * p = 0.0243; Spleen * p = 0.0332; 28 days PB ** p = 0.00035; BM *** p < 0.0001; Spleen ** p =0.0014).

E, Histological analysis of AML infiltration in the livers, spleens, and PB of mice after secondary transplant of WT and *lair1*-null AML cells at 4 weeks and 20 weeks (hematoxylin/eosin staining for livers and spleens, HEMA 3 staining for cytospin-prepared PB samples). Shown are representative images from at least three similar images. Scale bar is 100 μM.

F, Survival curves of mice transplanted with 1×10^5 pooled GFP^+ BM cells that were collected from primary recipients transplanted with WT or *lair1*-null AML1-ETO9a cells (n = 10 mice; p = 0.00012, log-rank test).

G, Percentages of AML1-ETO9a GFP^+ leukemia cells in BM at 1 month after secondary transplantation (mean ± s.e.m., Student's t-test; n = 10 mice; *** $p < 0.0001$).

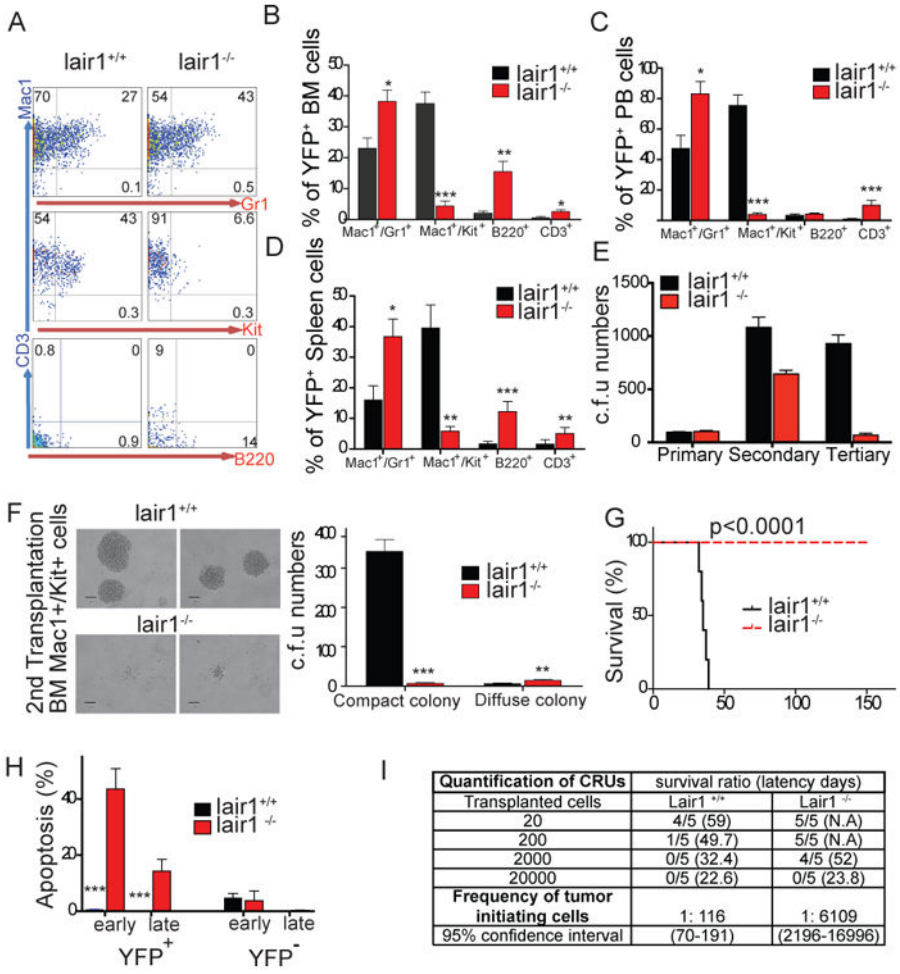

Quantification of CRUs	survival ratio (latency days)	
Transplanted cells	Lair1 +/+	Lair1 -/-
20	4/5 (59)	5/5 (N.A)
200	1/5 (49.7)	5/5 (N.A)
2000	0/5 (32.4)	4/5 (52)
20000	0/5 (22.6)	0/5 (23.8)
Frequency of tumor initiating cells	1: 116	1: 6109
95% confidence interval	(70-191)	(2196-16996)

Fig 4. LAIR1 deficiency exhausts tumor initiating cells by apoptosis

A, Representative flow cytometry plots showing that secondarily transplanted mice receiving *lair1*-null AML cells had markedly decreased percentages of $Mac1^+Kit^+$ cells and increased differentiated $B220^+$ and $CD3^+$ cells in YFP^+ compartments compared to mice receiving WT AML cells. Three pairs of mice were used for the comparison. B-D, Percentages of $YFP^+Mac\text{-}1^+Kit^+$, $YFP^+Mac\text{-}1^+Gr\text{-}1^+$, YFP^+B220^+, and YFP^+CD3^+ cells in (B) BM, (C) PB, and (D) spleen of secondary recipient mice transplanted with the WT or *lair1*-null MLL-AF9 AML cells at day 18 post-transplant (mean ± s.e.m., Student's t-test; n = 5 mice; (B) Mac1+/Gr1+ * p = 0.0195; Mac1+/kit+ ***p <0.0001; B220+ ** p = 0.0025; CD3+ * p = 0.0256; (C) Mac1+/Gr1+ * p = 0.0211; Mac1+/kit+ ***p <0.0001; CD3+ ***p <0.0001; (D) Mac1+/Gr1+ * p = 0.0342; Mac1+/kit+ **p =0.0015; B220+ *** p <0.0001; CD3+ ** p = 0.0027).

E, Comparison of colony-forming activity of WT and *lair1*-null MLL-$AF9^+$ BM cells during serial replating. Data from one experiment with n=3 technical replicate samples are shown. The experiment was repeated 3 times with similar results.

F, Left panel shows typical morphology of WT and *lair1*-null colonies formed by $YFP^+Mac\text{-}1^+Kit^+$ cells collected from secondarily transplanted mice at 28 days post-transplant. The right panel is a comparison of colony-forming activity of $Mac1^+Kit^+$ cells

from MLL-AF9$^+$ bone marrow cells harvested at 28 days after secondary transplantation. Scale bar is 10 μM. Data from one experiment with n=3 technical replicate samples are shown. The experiment was repeated 3 times with similar results.

G, Survival curve of tertiary recipient mice transplanted with 1,000 YFP$^+$Mac1$^+$Kit$^+$ cells from MLL-AF9$^+$ WT or *lair1*-null BM cells harvested at 28 days after secondary transplantation (n = 10 mice; p = 0.000022, log-rank test).

H, Flow cytometry analysis of apoptosis in mouse MLL-AF9 YFP$^+$ (AML) cells and YFP$^-$ (normal) cells. Early apoptosis was detected as Annexin V positive/PE positive/7-AAD negative staining and late apoptosis was detected as Annexin V positive/PE positive/7-AAD positive staining (mean ± s.e.m., Student's t-test; n =3 samples, *** p < 0.0001).

I, Limiting dilution assays comparing the frequencies of AML stem cells in WT and *lair1*-null MLL-AF9$^+$ AML. The indicated YFP$^+$ WT and *lair1*-null MLL-AF9$^+$ BM cells that were collected from primary recipients were co-transplanted with 2×10^5 bone marrow competitor cells into lethally irradiated recipients. The CRUs were calculated by L-Calc software.

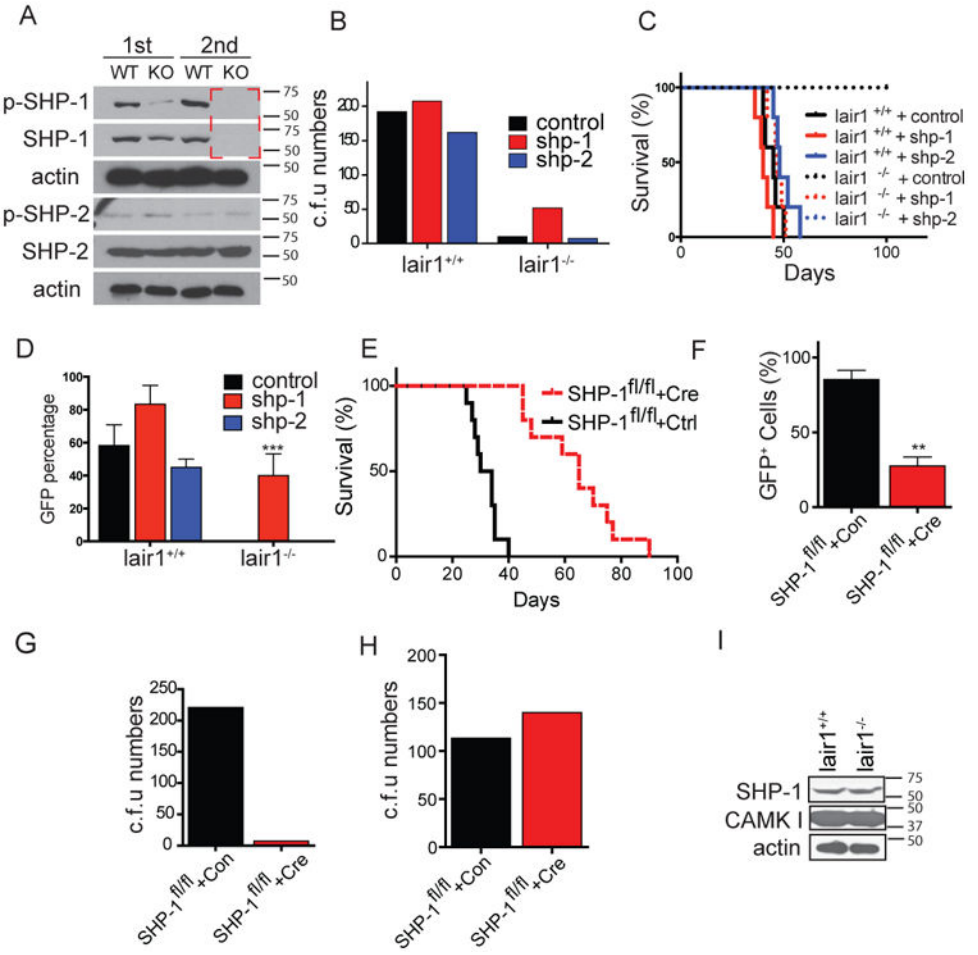

Fig 5. SHP-1 rescues the *lair1*-null AML phenotype

A, Phospho-SHP-1 and total SHP-1 levels in *lair1*-null and control MLL-AF9^{+} BM cells from both primarily and secondarily transplanted mice were determined by western blotting. The experiment was repeated for 5 times, which gave similar results.

B, Retrovirally-expressed SHP-1 increased CFU numbers of *lair1*-null AML cells compared to cells that were infected with control or SHP-2-expressing viruses in colony-forming assays. Retrovirally-expressed SHP-1 and SHP-2 had similar levels as endogenous proteins in WT controls.

C-D, Retrovirally-expressed SHP-1 rescued *lair1*-null phenotype upon tertiary transplantation. MLL-AF9^{+} WT or *lair1*-null BM cells in secondarily transplanted mice were harvested at 28 days and were infected by SHP-1 encoding or control virus. (C) Survival curves of mice transplanted with 3,000 of these ectopically SHP-1-expressing, SHP-2-expressing, or control cells (n= 5 mice; $p < 0.0001$, log-rank test). (D) Percentages of retrovirus-infected (GFP^{+}) AML cells in PB of tertiary recipient mice after 28 days of transplantation (mean ± s.e.m., Student's t-test; n =3 samples, *** $p < 0.0001$).

E-G, Bone marrow cells isolated from 5-fluorouracil pretreated SHP-1$^{fl/fl}$ mice were transformed with retroviral MLL-AF9 and then transduced by infection with empty vector or Cre-expressing vector to generate control (SHP-1$^{fl/fl}$ + Con) or SHP-1-deficient (SHP-1$^{fl/fl}$ + Cre) MLL-AF9 AML cells. (E) Survival curves of mice receiving 3,000 GFP^{+}

SHP-1$^{fl/fl}$ + Con or SHP-1$^{fl/fl}$ + Cre MLL-AF9 AML cells (n = 10; $p < 0.0001$, log-rank test). (F) Comparison of percentages of GFP^{+} AML cells in the PB from SHP-1$^{fl/fl}$ + Con and SHP-1$^{fl/fl}$ + Cre MLL-AF9 AML cells injected mice (mean ± s.e.m., Student's t-test; n = 10 mice; ** $p = 0.0067$). (G) Comparison of colony-forming abilities of SHP-1$^{fl/fl}$ + Con and SHP-1$^{fl/fl}$ + Cre MLL-AF9 AML cells.

H, Bone marrow cells isolated from 5-fluorouracil pretreated SHP-1$^{fl/fl}$ mice were transduced by infection with empty vector or Cre expression vector to generate control (SHP-1$^{fl/fl}$ + Con) or SHP-1-deficient (SHP-1$^{fl/fl}$ + Cre) cells without the MLL-AF9 transformation. Shown is the comparison of colony-forming abilities between control and SHP-1-deficient bone marrow cells.

I, Total SHP-1 and CAMK1 levels in WT and *lair1*-null BM cells were determined by western blotting.

In Fig. 5B, G, and H, data from one experiment with n=3 technical replicate samples are shown. The experiment was repeated 3 times with similar results.

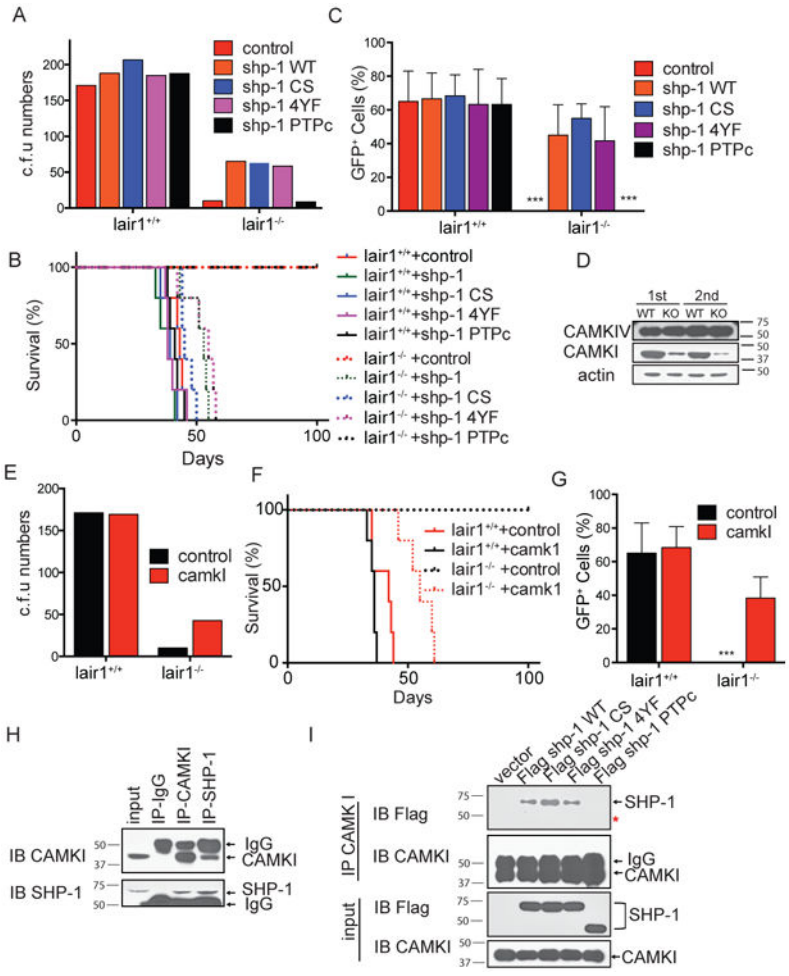

Fig 6. SHP-1 functions as an adaptor to recruit CAMK1 in the LAIR1 signaling

A, Retrovirally-expressed WT SHP-1 or mutants $C_{453}S$ or 4YF (278, 303, 538, 566), but not the SHP-1 PTP domain (PTPc), increased CFU numbers of *lair1*-null AML cells. Data from one experiment with n=3 technical replicate samples are shown. The experiment was repeated 3 times with similar results.

B-C, Retrovirally-expressed SHP-1 WT, $C_{453}S$, and 4YF, but not SHP-1 PTPc, rescued *lair1*-null phenotype upon transplantation. The green, blue, and purple dotted lines representing SHP-1 WT, $C_{453}S$, and 4YF virus infected leukemia BM cells reversed *lair1*-null MLL-AF9$^+$ leukemia development. The red dotted line representing control virus infected leukemia BM cells and black dotted line representing SHP-1 PTP domain virus infected leukemia BM cells were unable to rescue (n= 5 mice; (B) $p < 0.0001$, log-rank test; (C) *** $p < 0.0001$, mean ± s.e.m., Student's t-test).

D, Total CAMK1 and CAMK5 levels in *lair1*-null and control MLL-AF9$^+$ BM cells from both primarily and secondarily transplanted mice were determined by western blotting.

E, Retrovirally-expressed CAMK1 increased CFU numbers of *lair1*-null AML cells. Data from one experiment with n=3 technical replicate samples are shown. The experiment was repeated 3 times with similar results.

F-G, Retrovirally-expressed CAMK1 rescued *lair1*-null phenotype upon transplantation. MLL-AF9^{+} WT or *lair1*-null BM cells in secondarily transplanted mice were harvested at 28 days and were infected by CAMK1-encoding or control virus (n= 5 mice, (F) $p < 0.0001$, log-rank test; (G) *** $p < 0.0001$, mean ± s.e.m., Student's t-test).

H, Endogenous CAMK1 and SHP-1 interact with each other as determined by bi-directional pull down assays. WT MLL-AF9^{+} BM cells (1×10^{7} cells) were lysed by RIPA buffer, and indicated antibodies were used for immunoprecipition and western blot.

I, The C-terminal phosphatase-active domain of SHP-1 did not bind to CAMK1 in transfected 293T cells. The indicated Flag-tagged WT or mutant SHP-1 proteins were overexpressed in 293 cells. Flag antibody was used to precipitate SHP-1 proteins, and the Flag or CAMK1 antibodies were used in western blots.

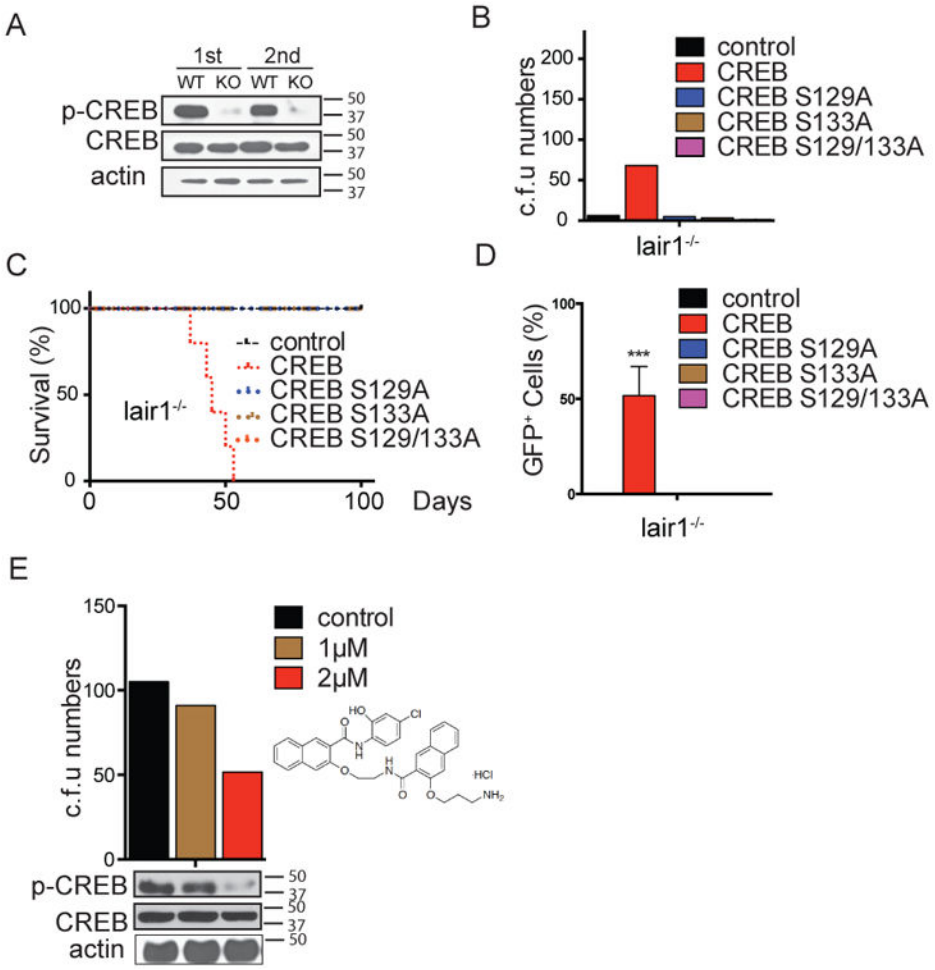

Fig 7. CREB is a transcription factor for LAIR1 signaling in AML cells

A, Phospho-CREB and total CREB levels in *lair1*-null and control MLL-AF9^{+} BM cells from both primarily and secondarily transplanted mice were determined by western blotting. B, Retrovirally-expressed CREB WT, but not CREB S129A, S133A, or S129/S133A, increased CFU numbers of *lair1*-null AML cells. Data from one experiment with n=3 technical replicate samples are shown. The experiment was repeated 3 times with similar results.

C-D, Retrovirally-expressed CREB WT, but not CREB mutants, rescued *lair1*-null phenotype upon transplantation. While the red dotted line representing CREB WT virus infected leukemia BM cells reversed the *lair1*-null MLL-AF9^{+} leukemia development, the black, blue, brown, and green dotted lines representing control, CREB S129A, CREB S133A, CREB S129/133A virus each infected leukemia BM cells were unable to do so (n= 5 mice; (C) $p < 0.0001$, log-rank test; (D) *** $p < 0.0001$, mean ± s.e.m., Student's t- test).

E, Treatment with a CREB inhibitor XX15 reduced CREB phosphorylation and the colony forming ability of WT AML cells. The molecule structure of the CREB inhibitor XX15 is shown. Data from one experiment with n=3 technical replicate samples are shown. The experiment was repeated 3 times with similar results.

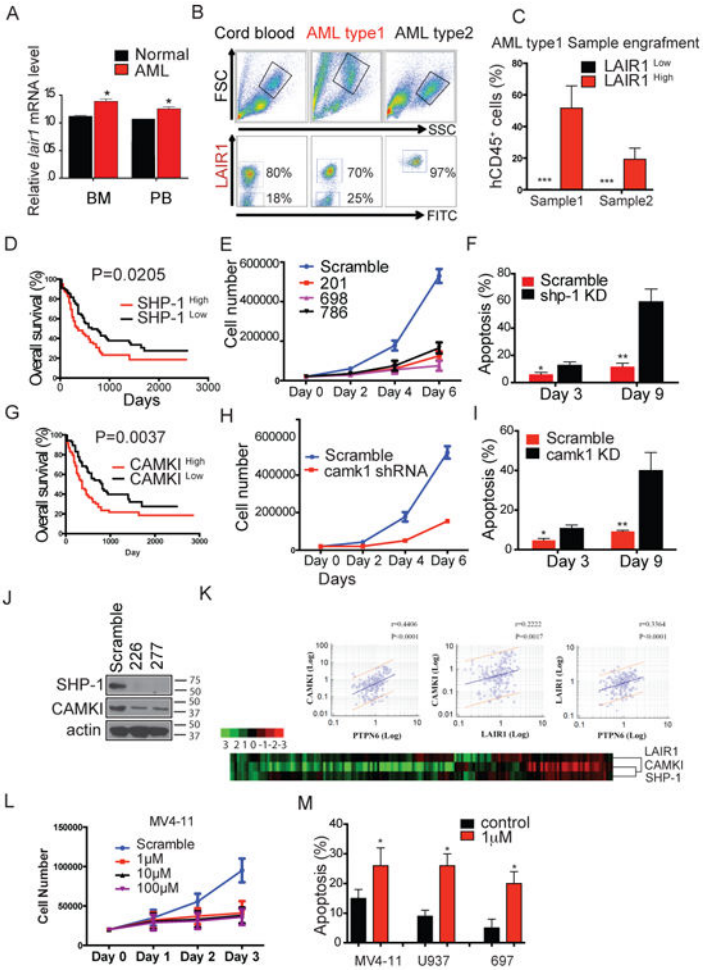

Fig 8. LAIR1 signaling is essential for human leukemia development

A, Expression of *lair1* mRNA differs significantly in BM and PB of AML patients (n = 7 BM or 19 PB respectively) from those in normal samples (n = 10 BM or 9 PB; mean ± s.e.m., Student's t-test; BM * p = 0.0329; PB * p = 0.0421).

B, Representative flow cytometry plots showing different LAIR1 expression patterns in normal mononuclear cells (Cord blood) and primary AML cells (type 1 and type 2). A representative plot of a flow cytometry analysis (from at least 3 similar images) of an type 1 sample shows that cells are present that express both high and low levels of LAIR1. Type 2 samples mainly contain $LAIR1^{high}$ cells. Data on these primary AML samples are listed in sTable 3.

C, Summary of percentages of $hCD45^{+}$ cells in PB of NSG mice transplanted with $LAIR1^{low}$ or $LAIR1^{high}$ primary human AML cells from 2 patient samples at 4 months after transplantation (mean ± s.e.m., Student's t-test, n= 5 mice, *** $p < 0.0001$).

D&G, Expression of *shp-1* or *camk1* mRNA negatively correlates with the overall survival of AML patients. n = 82 samples for high and n = 83 samples for low (TCGA database); (D) p =0.0205; (G) p =0.0037, log-rank test).

E&H, Treatment with shRNAs targeting *shp-1* or *camk1* inhibited the growth of MV4-11 cells.

F&I, Increased apoptosis in *shp-1*-silenced (by shRNA 698) or *camk1*-silenced MV4-11 cells (mean ± s.e.m., Student's t-test; n =3 samples, (F) Day 3 *p =0.0324; Day 9 ** p = 0.0019; (I) Day 3 *p =0.0302; Day 9 ** p = 0.0031).

J, Endogenous SHP-1 and CAMK1 expression was silenced with shRNAs (226, 277) in MV4-11 cells as determined by western blotting at 72 hours after shRNA-encoding lentiviral infection.

K, Expression of *lair1*, *camk1*, and *shp-1* in 165 AML patients (TCGA database) showed highly significant positive correlations. These correlations were also supported by clustering analysis.

L, CREB inhibitor XX15 treatment inhibited the growth of MV4-11 cells.

M, Flow cytometry analysis of apoptosis of MV4-11, U937, and 697 cells after one day of treatment with XX15 (mean ± s.e.m., Student's t-test; n =3 samples, MV4-11 *p =0.0411; U937 ** p = 0.0216; 697 *p =0.0294).

In Fig. 8E, H, and L, data from one experiment with n=3 technical replicate samples are shown. The experiment was repeated 3 times with similar results.